Published in final edited form as:

J Invest Surg. 2022 January ; 35(1): 111–118. doi:10.1080/08941939.2020.1829755.

Experimental modeling of necrotizing enterocolitis in human infant intestinal enteroids

Christie Buonpane[2], **Guillermo Ares**[2], **Carrie Yuan**[2], **Camille Schlegel**[1], **Heather Liebe**[1], **Catherine Hunter**[1,#]

[1]University of Oklahoma Health Sciences Center, Department of Surgery, Division of Pediatric Surgery, Oklahoma City, Oklahoma, OK 73104 USA

[2]Ann and Robert H. Lurie Children's Hospital of Chicago Division of Pediatric Surgery. 211 E Chicago Avenue, Box 63, Chicago, IL 60611 USA

Abstract

Experimental model systems are of paramount importance in advancing our understanding of human disease. There are several limitations when using a single cell culture to recapitulate the findings in a complex organism and results often vary between species, when proxy animal models are studied. Human enteroids have allowed for study of human disease in complex multicellular culture systems. Here we present the novel use of human infant enteroids generated from premature infant intestine to study necrotizing enterocolitis (NEC), which is a devastating intestinal disorder that affects our most vulnerable pediatric population. We demonstrate that NEC can be induced in premature human enteroids as supported by corresponding alterations in inflammation, apoptosis, tight junction expression, and permeability by treatment with lipopolysaccharide.

Keywords

NEC; enteroid; model; human; infant; tight junctions

Introduction

Intestinal organoids or enteroids, are described as three-dimensional spheroid intestines cultured *ex-vivo* from intestinal samples of biopsies. Enteroids develop from intestinal stem cells, and were first generated from mouse stem cells by Drs. Clevers and Sato [1]. A few years later, human enteroids were cultured by the same investigators [2–4]. This *ex-vivo* model has been an exciting advancement in allowing a system that, in part, recapitulates the multicellular complexity of the gastrointestinal tract. We and others, have grown enteroids from both adult and infant tissues as well as from different areas of the gastrointestinal tract [5–8]. This allows for analysis of interactions specific to certain tissues or intestinal locations.

[#]Corresponding author. Catherine J Hunter, MD., University of Oklahoma Health Sciences Center, Department of Surgery, 800 Stanton L. Young Blvd., Oklahoma City, Oklahoma, OK 73104 USA. Fax: 405-271-3919. Phone: 405-271-3677. chuntermd@gmail.com.

Enteroids model both structure and function while maintaining the genetic identity of the host.

Necrotizing enterocolitis is a devasting gastrointestinal disease that typically afflicts premature infants. As many as 7% of all infants admitted to the neonatal intensive care unit may develop this disease. NEC remains a leading cause of short gut syndrome. Although the definitive cause(s) of NEC remain unknown, contributing factors include an immature intestine and the presence of bacteria which remain important in the pathophysiology of disease. Many different animal models have been developed to study NEC, including rat, mouse and pig models. The ability to study this disease directly in humans is limited given the typical vulnerable patient population that is affected. Enteroids generated from the “at risk” population of premature infants present an especially important model of study for these patients. We hypothesized that enteroids generated from premature infants and treated with LPS would function as a useful and novel model of NEC. Herein, we present data supporting a novel human infant enteroid model of NEC.

Materials and Methods

Human Tissue

Following approval by the institutional review board approval (#2013-15152), discarded intestinal segments from infants undergoing surgical resection were collected. The tissues were collected from premature infants (ex 26-35 weeks). The age at time of collection ages ranged from 1 day to a corrected gestational age of 44 weeks. Informed consent from parents or the guardian were obtained. Tissue obtained from the operative suite were collected in Dulbecco’s Phosphate Buffered Saline (DPBS) (Thermo Fisher Scientific, Waltham, MA) prior to enteroid processing.

Enteroid Processing

The human tissue obtained from the operative suite was then utilized for enteroid processing within 24 hours. The full protocol has previously been published [5]. The specimen was cut into 0.5cm segments and placed in chelating buffer (15 min at 4°C). The specimen was filtered using a 100μm strainer. The tissue was placed in a second chelating buffer for the same duration. Tissue was then placed in cold DMEM (Gibco, Grand Island, NY) and shaken for 10 seconds. The tissue was filtered through a 100μm cell strainer. The flow through was strained with a 100 μm strainer. This was then centrifuged at 200 g for 15 minutes at 4°C. Following removal of the supernatant, the pellet and leftover supernatant were resuspended and centrifuged at 200 g for 20 minutes at 4°C. The supernatant and pellet were then resuspended in 500 μL of basement membrane matrix (Corning, Corning NY). The basement membrane and specimen mixture were placed in 50 μL aliquots in the center of a well in a 24-well plate until all used. The 24-well plate was placed in 37°C, 5% CO_2 incubator for 30 minutes to polymerize. 500 μL of Human Minigut Media Complete was added to each well and replaced every two days. Enteroids were collected when budding was visualized, typically at 5-10 days. Enteroids were imaged with Keyence BZ-X and buds were counted by averaging the number of buds per enteroid on high power field (40x).

Bacterial Strains and Reagents

Lipopolysaccharide (LPS) from *E. coli* strain 0111:B4 (Sigma, St. Louis, MO) was reconstituted in normal saline to a standard stock concentration (5mg/mL). We added 10 μL (5 mg/mL of LPS) to the enteroid media to induce experimental NEC.

Antibodies

The following primary antibodies were used for immunohistochemistry in this study: claudin-1 (rabbit polyclonal, Abcam 15098, 1:300 dilution), claudin-2 (mouse monoclonal, Thermo Fisher Scientific, 32-5600, 1:300 dilution), claudin-3 (rabbit polyclonal, Thermo Fisher Scientific, 34-1700, 1:300 dilution), claudin-4 (mouse monoclonal, Thermo Fisher Scientific, 32-9400, 1:300 dilution), occludin (mouse monoclonal, Thermo Fisher Scientific, 33-1500, 1:300 dilution), E-cadherin (rabbit monoclonal, Cell Signaling Technology, 24E10, 1:300 dilution) and ZO-1 (rabbit monoclonal, Cell Signaling Technology, D6L1E, 1:300 dilution).

Quantitative RT-PCR

Total RNA was extracted from enteroids using the RNeasy Mini Kit (Qiagen, Netherlands). The Nanodrop ND-1000 Spectrophotometer (NanoDrop Technologies Inc., Wilmington, DE) measured RNA concentration. cDNA was generated using GeneAMP RNA PCR Core Kit (Thermo Fisher Scientific, MA). Samples were analyzed by quantitative RT-PCR (Bio-Rad CFX and iQ SYBR Green Supermix). Primer sequences used: GAPDH: forward 5'-ACCACAGTCCATGCCATCAC-3', reverse 5'-TCCACCACCCTGTTGCTGTA-3', E-Cadherin: forward 5'-CTTTGACGCCGAGAGCTACA-3', reverse 5'-TTTGAATCGGGTGTCGAGGG-3', Claudin 1: forward: 5′-TGAGGATGGCTGTCATTGGG-3′, reverse: 5′-AAAGTAGGGCACCTCCCAGA-3′, Claudin 2: (Santa Cruz, Dallas, TX, # sc-62124-PR), Claudin 3: forward: 5′-GCCACCAAGGTC GTCTACTC-3′, reverse: 5′-CCTGCGTCTGTCCCTTAGAC-3′, Claudin 4: forward: 5′-GGCCGGCCTTA TGGTGATAG-3′, reverse: 5′-AGTAAGGCTTGTCTGTGCGG-3′, ZO-1: forward: 5'-AGGGGCAGTGGTGGTTTTCTGTTCTTT-3', reverse: 5'-GCAGAGGTCAAAGTTCAAGGCTCAAG-3', Occludin: forward: 5'-TCAGGGAATATCCACCTATCACTTCAG-3', reverse: 5'-CATCAGCAGCAGCCATGTACTCTTCAC-3', TLR4: forward 5'-TGCTCGGTCAGACGGTGATA-3', reverse 5'-TAGGAACCACCTCCACGCA-3', TNFa: forward 5'-CTCGAACCCCGAGTGACAAG-3', reverse 5'-TGAGGTACAGGCCCTCTGAT-3', IL1b: forward 5'-CTTCGAGGCACAAGGCACAA-3', reverse 5'-TTCACTGGCGAGCTCAGGTA-3'. Glyceraldehyde 3-phosphate dehydrogenase (GAPDH) was used to normalize results. Alterations in genes were measured as relative-fold changes and assayed with Bio-Rad CFX software (v. 3.0) by delta-delta CT calculations.

Immunofluorescence Microscopy

Following collection, we embedded the enteroids in paraffin. Sections were 4uM. Slides were baked for 1hour at 65°C. The paraffin was removed by using Safe Clear (Fisher Scientific, MA). Antigen retrieval was achieved by application and steaming with

eBioscience IHC Antigen Retrieval Solution. Thereafter, a cold PBS wash and blocking with 5% normal goat serum with 0.1% triton for 30 minutes was performed. The enteroids were then incubated overnight at 4°C with primary antibodies against claudin-1, claudin-2, claudin-3, claudin-4, occludin, E-cadherin or ZO-1. Subsequently slides were washed and incubated with a secondary antibody (1:1000 dilution) at room temperature for 1 hour. Slides were mounted with DAPI fluoroshield (Sigma, MO). All protocols were conducted according to the instructions. Fluorescent imaging was performed using the Nikon A1R multiphoton confocal microscope. Image analysis was performed using ImageJ.

Enteroid slides were treated according to the Apoptag Red In Situ apoptosis detection kit (MilliporeSigma, MA), using Safe Clear (Fisher Scientific, MA) to replace xylene washes. Slides were counterstained and mounted using DAPI fluoroshield (Sigma, St. Louis, MO). Apoptotic cells were visualized using the Nikon A1R Multiphoton microscope.

Permeability Assays

Permeability of enteroids were assessed after growth between 5-10 days on 24-well plates using Lucifer Yellow (Cat # L-453, ThermoFisher). Minigut media was gently removed from each well and enteroids were washed twice with 500uL PBS. Following wash, wells were replaced with 500uL of HBSS. 50uL of 2.5mg/mL Lucifer Yellow (10x dilution) were added to each well and incubated for 2 hours. Post incubation, HBSS was removed and enteroids were washed with PBS four times with gentle agitation. The number of enteroids per well was recorded to standardize between wells. Each well was then resuspended in 1000uL of PBS and vigorously pipetted up and down to lyse the enteroids. 100ul of the samples were measured in triplicate on a plate reader.

Statistical Analysis

Graphs and statistical analysis were performed using Graph Pad Prism 8. Statistical analysis was performed using parametric and non-parametric tests as appropriate. Statistical significance was accepted when $p<0.05$.

Results

Enteroids may be generated from intestinal samples from different gestational ages

A key experimental benefit of enteroids are that they may be generated from host tissue samples while maintaining the underlying genetics of the host. Enteroids may be generated from both full-term infants and premature infants. This is particularly important when developing a model to study the predisposition of the premature intestine to NEC. In Figure 1A, we show a photomicrograph of an intestinal sample taken from a premature infant undergoing a bowel resection from an atresia. Following processing, enteroids developed over a 7-day time course (Figure 1B). Hematoxylin and Eosin staining of a paraffin embedded enteroid reveals a polarized cystic structure with a luminal and basilar side. Period acid-Schiff (PAS) staining was used to show mucosubstances including glycoproteins, mucins, and goblet cells, while actin staining shows the structure of the cytoskeleton (Figure 1C).

Enteroids from premature infants treated with LPS demonstrate NEC-like features

Toll-like receptor 4 (TLR-4) is a transmembrane receptor that recognizes LPS and is increased in humans with NEC. Indeed, TLR4 receptor expression within the intestinal epithelium may contribute to the classic inflammatory reaction of the premature intestine to NEC. To determine the responsiveness of enteroids from premature infants to LPS and assess the expression of signature NEC-like features, gene expression analysis for TLR-4 was performed on both controls and LPS-enteroids (Figure 2A). Similar to human disease we found an increase in TLR-4 expression. Human NEC is also associated with a decrease in restitution and repair of the intestinal epithelium. To test these responses in the NEC-enteroid model, we counted budding as a measure of crypt survival. NEC-enteroids demonstrated significantly decreased budding compared with controls (Figure 2B). An increased inflammatory response is also a hallmark feature of NEC. To determine the cytokine response of the NEC-enteroid model we assayed cytokines characteristic of NEC, namely TNF-α and IL-1β, both of which demonstrated a significant increase as compared with controls (Figure 3A). Increased apoptosis was also shown to be increased by immunofluorescent staining in NEC enteroids vs. controls which are comparable with our findings in human disease (Figure 3B).

Tight junction differences are seen in a human enteroid NEC model

In order to recapitulate a NEC-like model in human enteroids generated from premature tissue, we treated human-derived enteroids with LPS and compared with non-treated enteroids (generated from the same host tissue). Human-derived enteroids demonstrate staining of junctional proteins including occludin, E-cadherin, zonula occludens (ZO-1) and claudins. However, enteroids treated with LPS showed decreased staining of these critical junctional proteins as seen in Figure 4A. RT-PCR was performed to assay junctional gene expression. A significant downregulation was noted in occludin and E-cadherin, which matches previously published findings in humans [9]. When premature human enteroids were treated with LPS, we also identified an increase in expression of the pore forming tight junction protein claudin- 2 in experimental NEC-enteroids (Figure 4B). This is similar to the results we have previously demonstrated in human NEC [10].RT-PCR further demonstrated an upregulation of claudin-2 in the NEC-enteroid model compared with controls (Figure 2B). Furthermore, a significant increase in permeability was also visualized in the NEC-enteroids when stained with Lucifer yellow (Figure 4C).

Discussion

The intestinal epithelium is a complex environment composed of many different cellular subtypes. The study of its intricate structure and function is of particular interest in understanding the pathophysiology of NEC. Multiple NEC models have been successfully developed to this goal. However, single-cell models fail to reproduce the complex interaction between the various intestinal types of cells. Likewise, animal models also have their shortcomings in recreating all relevant features of human NEC [11]. Enteroids have emerged as a unique system that combines the study and manipulation of human tissue in a multicellular culture that retains native architecture and function. As such, several authors have used enteroids to study the intestinal response to infectious diseases and the

pathophysiology of inflammatory bowel disease [12]. Indeed, enteroids are a useful tool to study human disease, and their use to study host-environmental interactions are increasing.

The development of age-relevant human models to study human intestinal disorders is particularly valuable to pediatric researchers. Although ninety percent of cases of NEC occur in infants who are born prematurely, the vast majority of premature infants do not develop NEC. Therefore, it is imperative that we have age-specific models to investigate the role of premature tissue as a catalyst in NEC. In addition to growing enteroids from premature tissue, we have also generated enteroids from infants with NEC. However, the technical aspects of this are challenging due to the general inflammation and injury of those specimens. The majority of infants with NEC do not require surgical resection. Of those who do, the amount of bowel resected is minimized in order to avoid future complications of short gut syndrome. Thus, tissue availability from babies with NEC is limited, creating a need for a premature NEC-enteroid model.

In this study, we propose the use of LPS to generate a NEC-like enteroid. Prior work by others on mouse enteroids have shown that LPS could reduce enteroid proliferation and that breast milk was a protective strategy against LPS-induced injury to enteroids. These results are also similar to what we find in human NEC, where breast milk is lauded as a protective strategy. Pharmaceuticals agents have been studied using LPS-induced injury in a rat enteroid model [13]. Although bacteria have been used in co-culture models of enteroid and organoid infection, no single organism meets Koch's postulates in the pathophysiology of NEC. However, the majority of positive cultures in patients with NEC are members of the Enterobacteriaceae family. This group includes a large family of gram-negative bacteria such as Escherichia coli, Enterobacter and Citrobacter, and these pathogens have key virulence factors, including the presence of LPS on their cell wall. Taken together these findings were the basis of utilizing LPS in our premature enteroid model of NEC.

The intestine is critical in the provision of host defenses and the maintenance of barrier integrity against pathogens. There is substantial evidence supporting that the intestinal epithelium is dysfunctional in NEC, leading to barrier breakdown, increased intestinal permeability, and bacterial translocation[14]. In this study, we have shown that human enteroids generated from premature intestine samples and treated with LPS, produce similar characteristic findings to human NEC. We found an upregulation of toll-like receptor 4 expression as well as the inflammatory cytokines TNF-alpha and IL-1Beta, which we used to validate our model since these markers been strongly linked to the pathogenesis of human NEC [15]. Functionally, the NEC-like changes induced by LPS injury led to the epithelial barrier dysfunction as quantified by increased permeability. Epithelial injury was further characterized in the enteroid model as decreased villous-crypt formations or "budding" of the enteroids. Budding and crypt fission is observed in healthy, proliferating organoids. Ultimately, these changes led to increased apoptosis of our enteroids, as is the expected terminal pathway in NEC[16].

Our previous work had demonstrated that changes in tight junction proteins are associated with the experimental NEC and may be responsible for alterations in permeability [9,10]. The enteroid NEC model exhibited similar variations in tight junction proteins. We found a

decrease in E-cadherin and occludin, which is thought to have protective barrier function. Additionally, we found increased expression of claudin-2 in the luminal aspect of the enteroids. This study lays the foundation of using premature human enteroids as a model for NEC, however, future work is needed to further enhance this model. Given that NEC is a multifactorial disease, introducing hypoxia or hypothermia to further mimic the hypoxic induced intestinal injury will likely strengthen this model and its applications.

Taken together, these findings support that LPS-treated enteroids grown from premature human bowel represent a useful tool in the study of NEC. The ability to study simultaneously architectural changes in a multicellular environment with the 3-dimensional architecture of the target organ is one of the most thrilling features of the human enteroid NEC-like model. As we look to the future, hopefully this model's applicability extends beyond understanding pathogenesis and into testing potential therapeutic pharmaceuticals and gene-modulators *ex vivo* for validation prior to human trials.

References:

1. Sato T, Vries RG, Snippert HJ, et al. Single Lgr5 stem cells build crypt-villus structures in vitro without a mesenchymal niche. Nature. 2009;459(7244):262–265. doi: 10.1038/nature07935 [doi]. [PubMed: 19329995]
2. Sato T, Clevers H. SnapShot: Growing organoids from stem cells. Cell. 2015;161(7):1700–1700.e1. doi: 10.1016/j.cell.2015.06.028 [doi]. [PubMed: 26091044]
3. Sato T, Clevers H. Growing self-organizing mini-guts from a single intestinal stem cell: Mechanism and applications. Science. 2013;340(6137):1190–1194. doi: 10.1126/science.1234852 [doi]. [PubMed: 23744940]
4. Sato T, Stange DE, Ferrante M, et al. Long-term expansion of epithelial organoids from human colon, adenoma, adenocarcinoma, and barrett's epithelium. Gastroenterology. 2011;141(5):1762–1772. doi: 10.1053/j.gastro.2011.07.050 [doi]. [PubMed: 21889923]
5. Ares GJ, Buonpane C, Yuan C, Wood D, Hunter CJ. A novel human epithelial enteroid model of necrotizing enterocolitis. J Vis Exp. 2019;(146). doi(146):10.3791/59194. doi: 10.3791/59194 [doi].
6. Drucker NA, McCulloh CJ, Li B, Pierro A, Besner GE, Markel TA. Stem cell therapy in necrotizing enterocolitis: Current state and future directions. Semin Pediatr Surg. 2018;27(1):57–64. doi: S1055-8586(17)30147-6 [pii]. [PubMed: 29275819]
7. Fujii M, Matano M, Toshimitsu K, et al. Human intestinal organoids maintain self-renewal capacity and cellular diversity in niche-inspired culture condition. Cell Stem Cell. 2018;23(6):787–793.e6. doi: S1934-5909(18)30552-6 [pii]. [PubMed: 30526881]
8. Almeqdadi M, Mana MD, Roper J, Yilmaz OH. Gut organoids: Mini-tissues in culture to study intestinal physiology and disease. Am J Physiol Cell Physiol. 2019;317(3):C405–C419. doi: 10.1152/ajpcell.00300.2017 [doi]. [PubMed: 31216420]
9. Grothaus JS, Ares G, Yuan C, Wood DR, Hunter CJ. Rho kinase inhibition maintains intestinal and vascular barrier function by upregulation of occludin in experimental necrotizing enterocolitis. Am J Physiol Gastrointest Liver Physiol. 2018;315(4):G514–G528. doi: 10.1152/ajpgi.00357.2017 [doi]. [PubMed: 29927318]
10. Ares G, Buonpane C, Sincavage J, Yuan C, Wood DR, Hunter CJ. Caveolin 1 is associated with upregulated claudin 2 in necrotizing enterocolitis. Sci Rep. 2019;9(1):4982–4. doi: 10.1038/s41598-019-41442-4 [doi]. [PubMed: 30899070]
11. Ares GJ, McElroy SJ, Hunter CJ. The science and necessity of using animal models in the study of necrotizing enterocolitis. Semin Pediatr Surg. 2018;27(1):29–33. doi: S1055–8586(17)30139–7 [pii]. [PubMed: 29275813]
12. Leber A, Hontecillas R, Tubau-Juni N, Zoccoli-Rodriguez V, Abedi V, Bassaganya-Riera J. NLRX1 modulates immunometabolic mechanisms controlling the host-gut microbiota interactions

during inflammatory bowel disease. Front Immunol. 2018;9:363. doi: 10.3389/fimmu.2018.00363 [doi]. [PubMed: 29535731]

13. Chen CL, Yu X, James IO, et al. Heparin-binding EGF-like growth factor protects intestinal stem cells from injury in a rat model of necrotizing enterocolitis. Lab Invest. 2012;92(3):331–344. doi: 10.1038/labinvest.2011.167 [doi]. [PubMed: 22157721]
14. Guo S, Nighot M, Al-Sadi R, Alhmoud T, Nighot P, Ma TY. Lipopolysaccharide regulation of intestinal tight junction permeability is mediated by TLR4 signal transduction pathway activation of FAK and MyD88. J Immunol. 2015;195(10):4999–5010. doi: 10.4049/jimmunol.1402598 [doi]. [PubMed: 26466961]
15. Hackam DJ, Afrazi A, Good M, Sodhi CP. Innate immune signaling in the pathogenesis of necrotizing enterocolitis. Clin Dev Immunol. 2013;2013:475415. doi: 10.1155/2013/475415 [doi]. [PubMed: 23762089]
16. Neal MD, Sodhi CP, Jia H, et al. Toll-like receptor 4 is expressed on intestinal stem cells and regulates their proliferation and apoptosis via the p53 up-regulated modulator of apoptosis. J Biol Chem. 2012;287(44):37296–37308. doi: 10.1074/jbc.M112.375881 [doi]. [PubMed: 22955282]

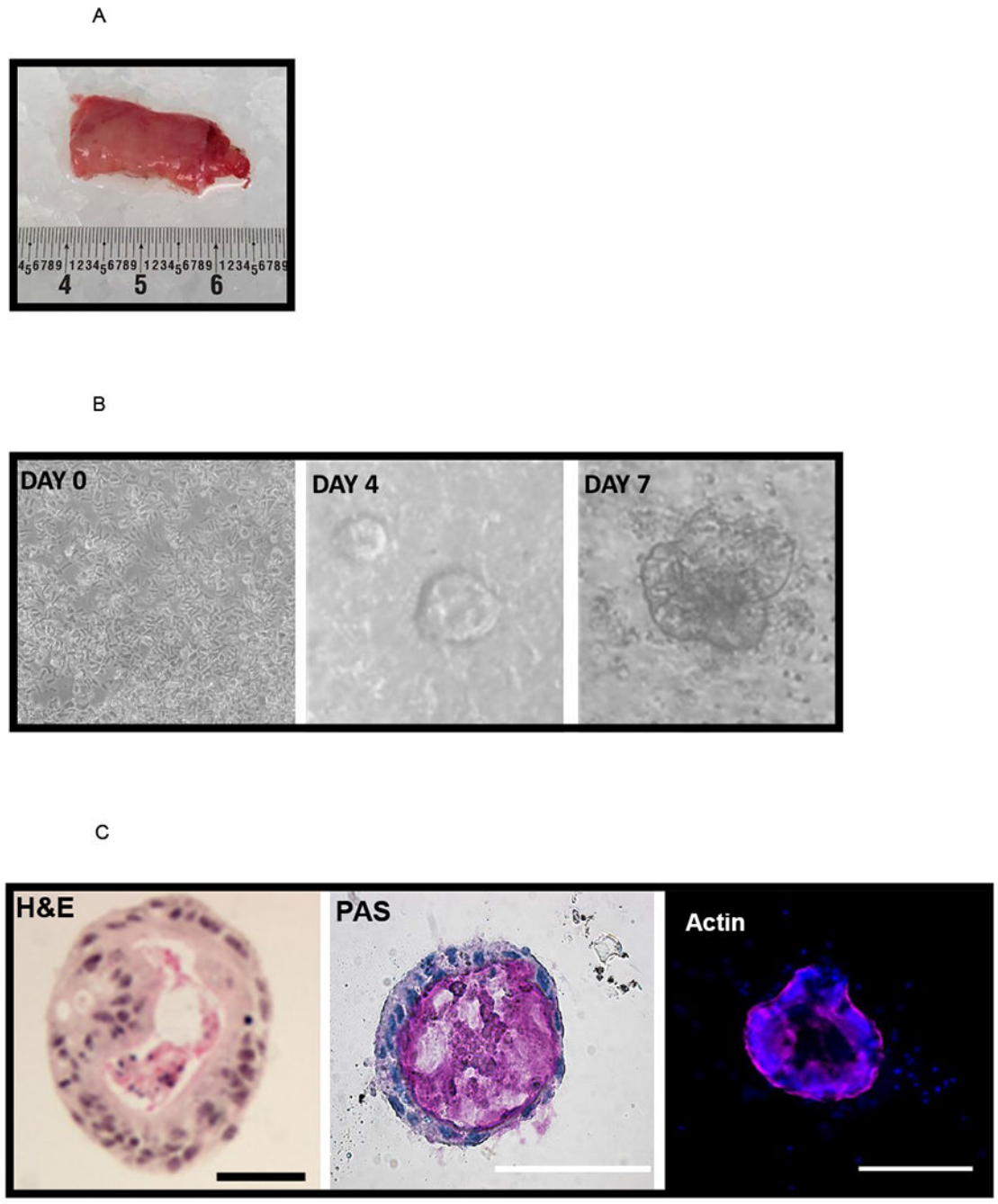

Figure 1.

[A] Discarded intestinal segments are collected at the time of surgery. A piece of neonatal ileum is shown. The anatomic location is noted, and the specimen is immediately placed on ice. Samples are processed as described in the methods.

[B] Crypt isolation and culture leads to generation of human enteroids. On day 0 a crypt culture shows characteristic cells with numerous rod-shaped cells, and by day 4 sphere-like enteroids can be seen. The day 7 enteroid is well developed with budding features. Experiments were repeated in triplicate with enteroids generated from 4 different samples.

[C] Structural appearance of the enteroids. The histological appearance is demonstrated by staining with hematoxylin and eosin. A central lumen is seen, encompassed by a polarized exterior. The nuclei are dark and the cytosol is pink. Goblet cells are present and staining with PAS reveals mucin (pink) within the center of the enterocyte. Experiments were repeated in triplicate with enteroids generated from four different samples. Immunofluorescence reveals the actin cytoskeleton (pink) and nuclei (blue + DAPI). Scale bar 50 μm.

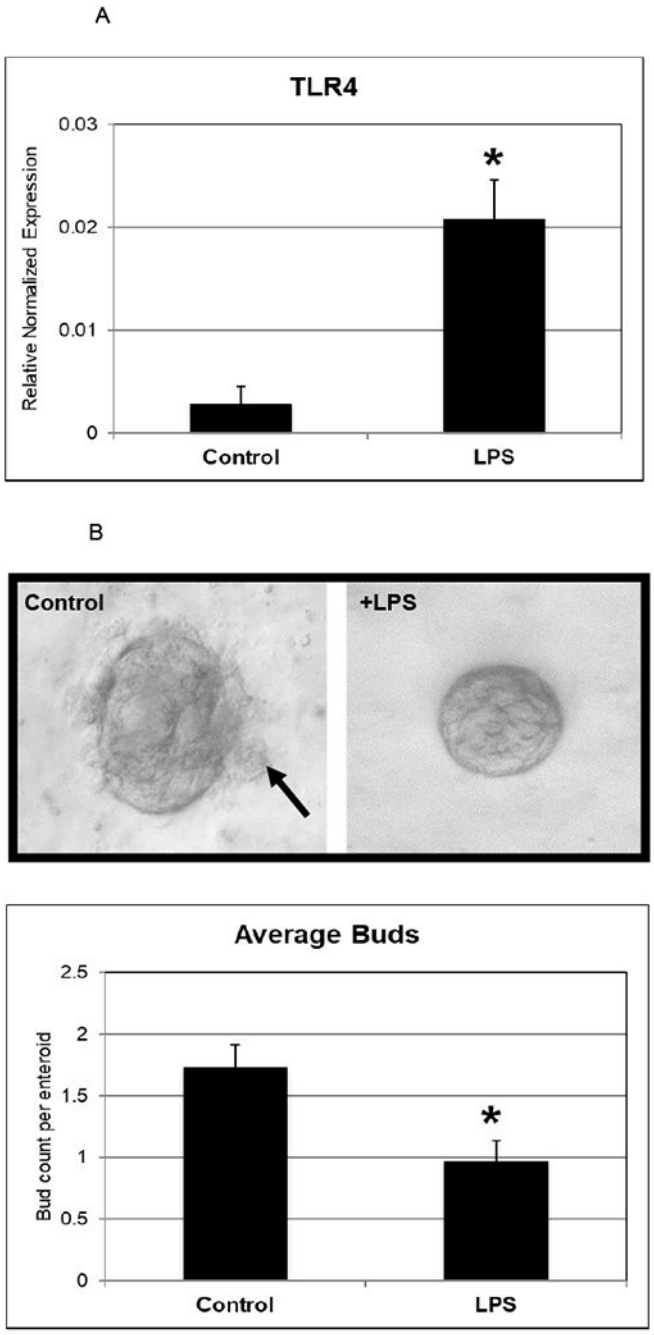

Figure 2.

[A] Human enteroids treated with LPS demonstrate molecular and structural changes that are similar to NEC. Upregulation of TLR-4 has been reliably shown to occur in human NEC. Day 5 enterocytes treated with LPS were shown to have an increase in RNA expression of TLR-4 ($p=0.03$). Values are +/− SEM with 6 samples per group.

[B] LPS decreases the amount of budding in enterocytes. Buds (black arrow) are seen on the control enterocyte at Day 6, whereas the LPS treated enterocyte is smooth appearing. Bud counts were performed and a significant decrease was noted (N = 30 in each group,

p=0.003). These experiments were repeated with enteroids generated from two different patient samples.

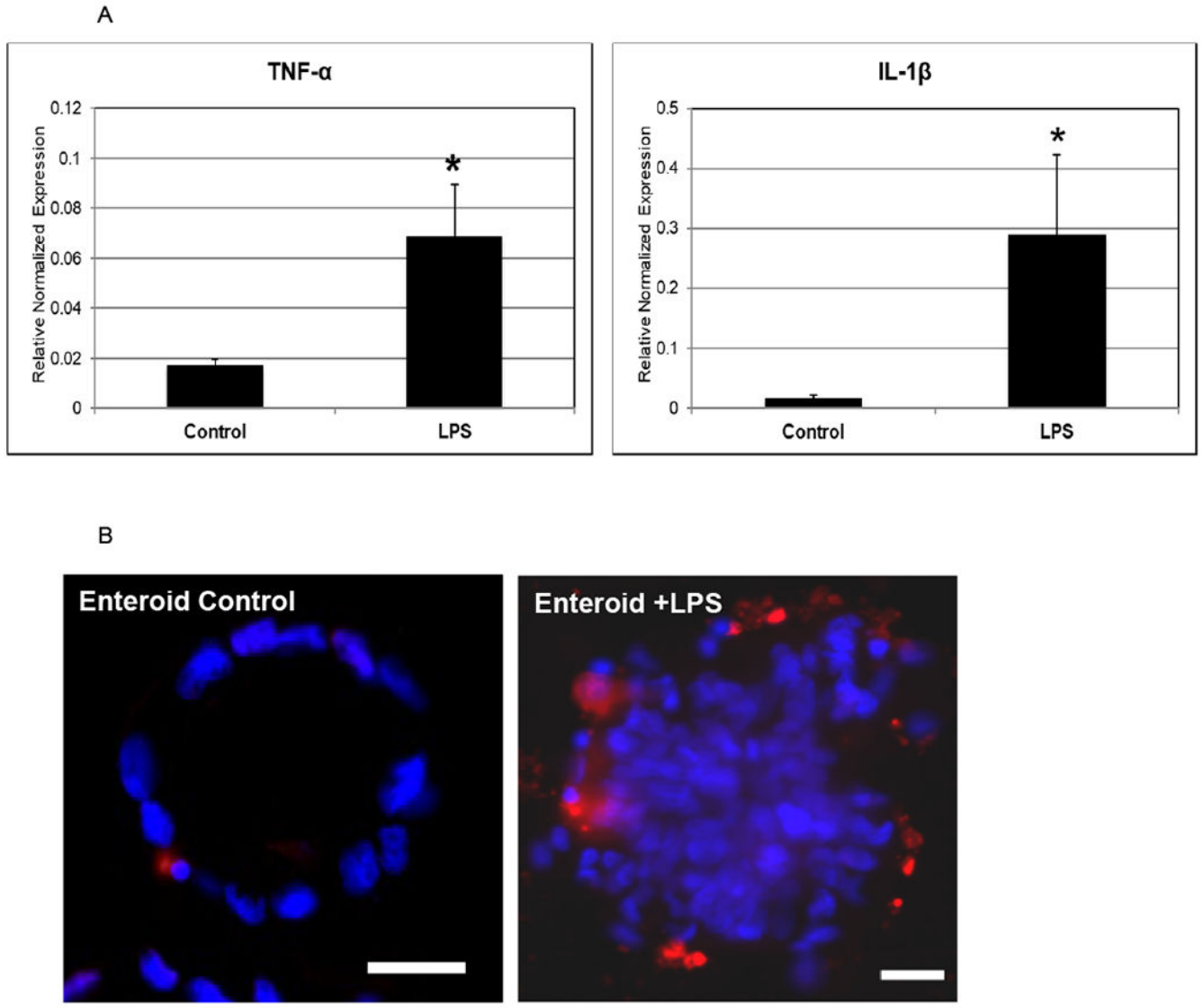

Figure 3.

[A] An increase of TNF-α and IL-1β are described in human NEC. RT-PCR demonstrates a robust increase in the expression of these cytokines ($p= 0.04$ and $p= 0.07$, respectively). This was repeated in triplicate.

[B] Increased intestinal epithelial apoptosis occurs in NEC. We demonstrate an increase in apoptosis in enterocytes treated with LPS. The control enterocytes have few apoptotic (red) cells, while the LPS treated enterocytes have many more apoptotic cells. The nuclei are stained with DAPI (blue). Scale bar 50 μm.

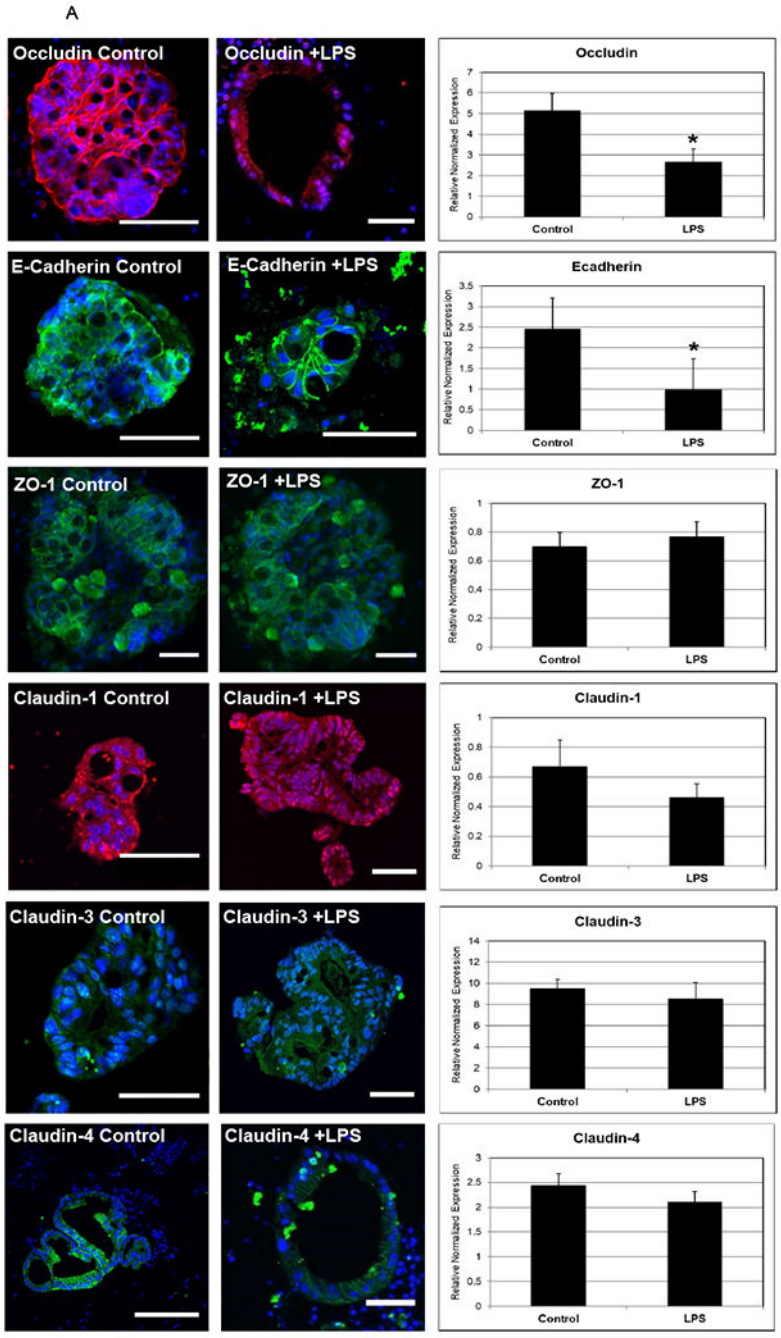

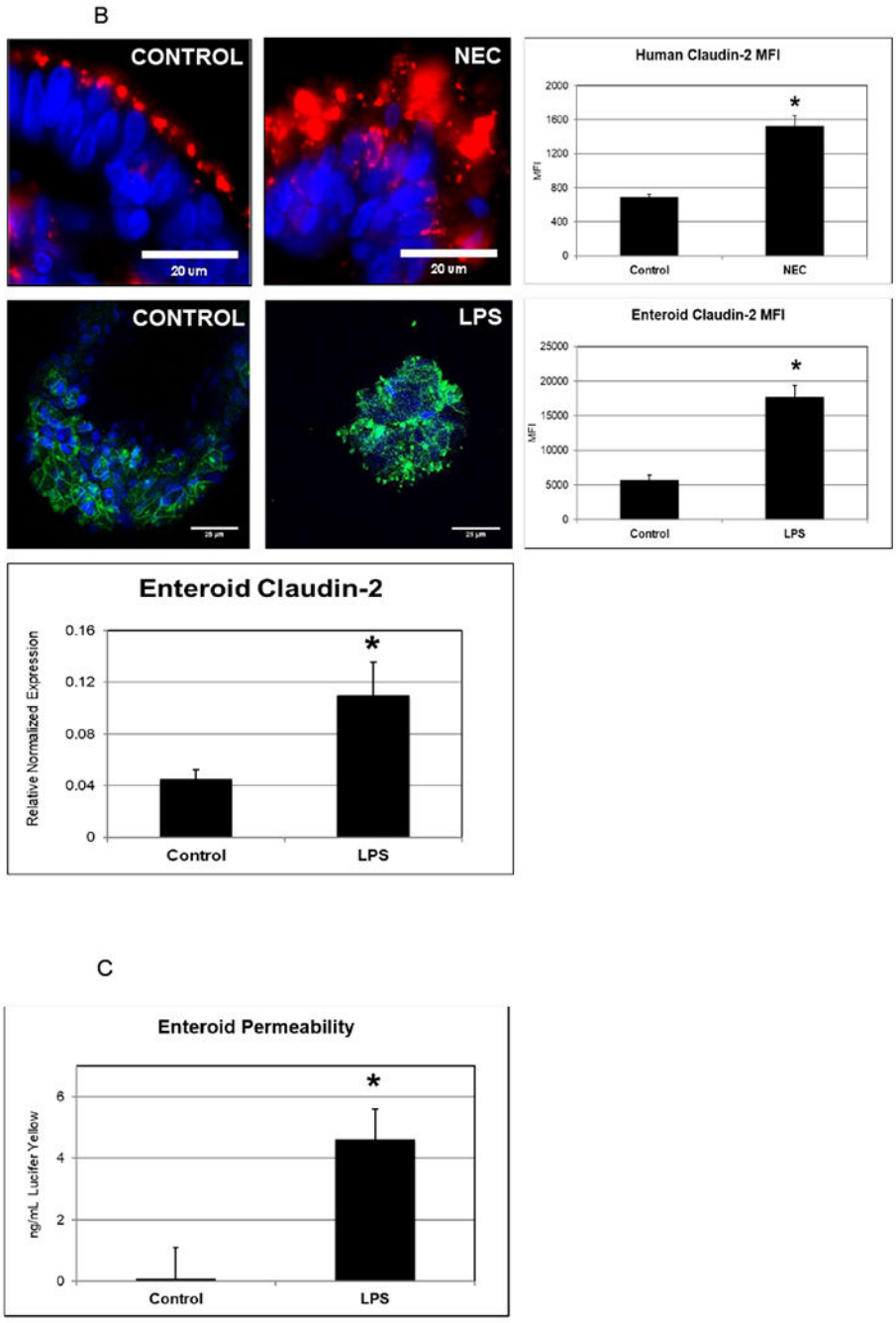

Figure 4.

[A] Enterocytes are polarized structures that express junctional proteins. Immunofluorescence was performed and demonstrated junctional protein changes between control and LPS conditions. In addition, RT-PCR was performed to assay gene expression of junctional proteins in response to LPS. Occludin protein (red) and gene expression was significantly decreased following LPS treatment (p=0.02) and E-cadherin (green) was also significantly decreased (p=0.03). ZO-1 (green), claudins 1 (red), 3 (green) and 4 (green) protein and gene expression appeared relatively unchanged after 24 hours of LPS treatment.

Nuclei are stained with DAPI (blue). At least three enterocytes were assayed per group. Scale bar 50 μm.

[B] Claudin-2 is upregulated in NEC and in human enterocytes treated with LPS. The upper panels show human ileum stained with DAPI (nuclei) and claudin-2 (red). In control human intestinal samples claudin-2 is located at the apical aspect of the epithelium. In patients with NEC, there is a more diffuse and increased protein expression of claudin-2. The lower panels demonstrate similar findings in human enterocytes (claudin 2 is stained green). Mean fluorescent intensity of claudin-2 was measured in both humans and enterocytes and found to be significantly higher in NEC/LPS ($p<0.0001$ and $p<0.0001$, respectively. An n value of 20 each was used. Additionally, a corresponding increase in the gene expression of claudin-2 in enterocytes ($p=0.04$) are noted.

[C] NEC is characterized by a loss of normal intestinal barrier integrity. Human enterocytes were treated with LPS, and after 24 hours permeability to Lucifer yellow was assayed. This was performed in triplicate. A significant increase in permeability was noted ($p<0.0001$).